Responses to Reviewers for: ***Developing A Custom-Built Metal Aerosol Processing Chamber: Analysis of Aerosol Coagulation at Low Humidities.***

Nevil A. Franco, Kyle J. Gorkowski, Katherine B. Benedict

Earth and Environmental Science Division, Los Alamos National Laboratory, P.O. Box 1663
Los Alamos, NM, US 87545-1663

Responses to the reviewers are shown in blue. **Additions to the main text are bold.**

Reviewer 2-

General Comment: Experimental facility presented in this manuscript is primarily aimed to understand wall-loss and coagulation processes of aerosols under controlled temperature and humidity conditions. Such facility holds potential to improve understanding of aerosol-processes in the atmosphere as well as improving cloud-chamber. However, this facility in current stage lacks temperature and humidity control. Since current set-up and any results presented here do not involve cloud-microphysical processes like CCN activation or cloud-droplet formation, it is not appropriate to consider this facility as a cloud-chamber.

This paper describes the experimental facility, data processing, parameter fitting in details and discuss wall-loss and coagulation factor for different aerosols, by fitting observations into loss equation. Although it has significant uncertainty, studies highlight that soot particles adhere to each other, more than others in dry conditions. I have few concerns regarding set-up and data processing. Hence, I would recommend reject and resubmit when more results are available, along with addressing major and minor comments listed below.

We would like to thank reviewer two for their comments. We agree that calling the chamber a "cloud chamber" was probably a step too far at this point in its development. Therefore, we have changed the title and references to the chamber to an "aerosol-processing chamber". The characterization of the chamber, without humidity and temperature control is still valuable, since the chamber is currently being used in dry conditions to determine the charge distribution of dust and we expect future experiments to be performed under similarly dry conditions. We have responded to each point below and made changes in the text to strengthen the manuscript and conclusions.

Major Comments

Comment 1: Authors emphasize that this facility is specifically designed to investigate coagulation processes of aerosols under different conditions (line 61-63). Further, authors have

not shown any results which deal with cloud-microphysical processes like CCN activation or presence of cloud droplets. Under such limitations, it is inappropriate to call the facility as ”cloud chamber”, which appears in title, abstract and few paragraphs. Since, it mostly deals with aerosol-processes, it should be referred to as an aerosol-processing chamber.

Response: We have made the suggested change throughout the manuscript.

Comment 2: Line 17-19: Uncertainty in the fitted coagulation factor, especially for sodium chloride and sucrose is too large to conclude that soot particles adhere to each other more than others. Conclusion does not seem robust considering this uncertainty level. It needs additional observation and analysis to reduce uncertainty.

Response: We have changed it to say that the average is different, but the uncertainty is high. The uncertainty largely comes from the accuracy of the SMPS (~20%). We have tried a variety of fitting and averaging (as the reviewer notes below) to improve the uncertainty but no large improvements were found. To further explore this area and help with future studies we have added Monte Carlo error analysis to assess the percent error one would expect. We add this new section to the main text.

Text added to manuscript:

4.4 Monte Carlo Error Analysis

To understand the large standard deviations that emerged from our fits of wall-loss and coagulation correction, we performed a Monte Carlo error analysis. We began by constructing three number-size distributions, each formed by the sum of two log-normal modes with equal particle numbers. In the first case, both modes were centered at 100 nm but differed in geometric standard deviation, i.e., the distribution is the summation of a 100 nm mode with a GSD of 1.4 plus a 100 nm mode with a GSD of 1.8. This summation of two log-normal distributions reflects the broad distributions we observe in our measurements. The second case repeated this structure at 200 nm. The third case was a hypothetical experiment that combined narrow 100 nm and 300 nm modes (both GSD = 1.2) to test the response to a bi-modal aerosol distribution.

For every distribution we calculated Equation 1 assuming a wall-eddy diffusivity of 0.1 s^{-1} and a coagulation correction factor (W_C^{-1}) of 1.0. This is a null case in which no additional correction to the Brownian coagulation kernel is required. We then superimposed random noise of ±20 % on both the size spectrum and the rate. This noise mirrors uncertainties reported in instrument intercomparisons of ±10 % error between 20 nm and 200 nm and up to ±30 % above 200 nm (Wiedensohler et al., 2012). Thus, ±20 % is a middle point

across the range we measured. Applying the same noise to the rate represents the best-case scenario for our analysis pipeline.

With these noisy data sets created, we refit the wall-eddy diffusivity and coagulation correction 80 times at each total number concentration shown in Figure 6. From the ensemble of fits we calculated the percent error in each retrieved parameter and averaged the results.

The results in Figure 6 reveal a clear trend percent error. When total number concentration exceeds roughly 10^4 cm^{-3}, the uncertainty in the coagulation correction begins to fall. This is consistent with the fact that Brownian coagulation scales with particle number squared and becomes distinguishable from measurement noise only at higher concentrations. Conversely, the error in the wall-eddy diffusivity grows with concentration. Once coagulation dominates the particle loss budget, the data contains too little information to constrain the comparatively low wall-loss sink, increasing the relative uncertainty. In other words, when coagulation governs the system dynamics, the wall-loss term becomes a minor, poorly resolved correction.

The three analyzed distributions exhibit similar percent errors in the coagulation correction. The slightly lower error for the 100 nm mode compared to the 200 nm mode is consistent with the behavior of the Brownian coagulation kernel, where smaller particles have higher coagulation coefficients and therefore undergo more frequent collisions. This leads to a greater rate of change in the distribution for a given number concentration, resulting in better signal-to-noise. The hypothetical bi-modal distribution generally shows the lowest uncertainty among the three cases (in our experimental range), although the improvement is modest.

Annotations in Figure 6 mark the concentration ranges for the three chamber experiment series: sucrose, NaCl, and smoke aerosols. They also indicate the measured coefficient of variation in the mean coagulation correction for each case. The agreement between these annotated uncertainties and the Monte Carlo error analysis confirms that the observed variability is consistent with the measurement noise.

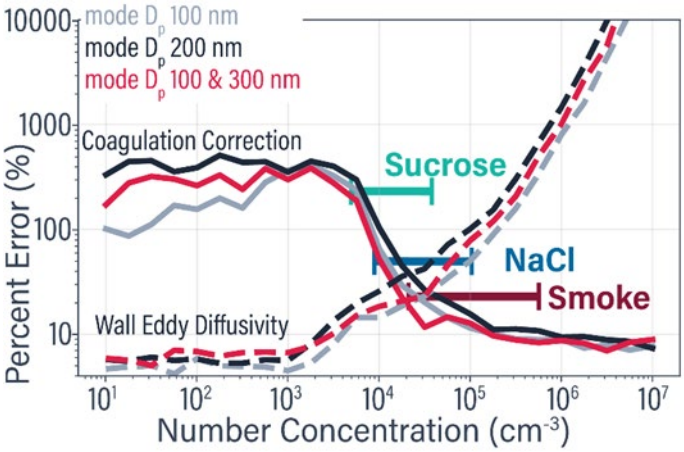

Figure 6: Percent error in fitting of coagulation correction (solid line) and wall-eddy diffusivity (dashed line) as a function of number concentration. Lines represent mean errors for size distributions with different modal diameters: 100 nm (gray), 200 nm (black), and a bi-modal 100 & 300 nm distribution (red). Annotated markers indicate representative number concentration ranges for sucrose, NaCl, and smoke experiments, along with the coefficient of variation (standard deviation divided by the mean) in the coagulation correction, reflecting relative uncertainty rather than bias.

Comment 3: Line 67-69: This study is also aimed to refine further experimental design. However, it has not been discussed the way it will help?

Response: The text added on the Monte Carlo error analysis, addresses this comment as that can be used to target the experimental conditions with lowest uncertainty for the parameters of interest. We have also updated the text to remove the specific statement about refining experimental design.

This section now reads: **Through this study, we aim to characterize the behavior of aerosol in the dry chamber (influence of particle composition and shape) and determine conditions suitable for future studies at elevated humidity including supersaturation. In addition, we perform an uncertainty analysis on the coagulation correction retrieval to determine the range of aerosol concentrations that reduce uncertainty in coagulation corrections.**

Comment 4: Line 133-138: Authors have used multiple minimization methods for fitting the size distribution each time step. Are methods same at each time-step? Do they change with aerosol species? Which methods have performed better?

Response: We have added additional details to this section to clarify. The following text was added: **We took this approach since the best fit varied with concentration and shape of the distribution. L-BFGS-B was typically the best for a lognormal distribution, but as the mode became broader (lower concentrations) then TNC, SLSQP or trust-constr would do better. The transition of when this would occur was not an obvious threshold. Therefore, we used all of these optimization routines for each lognormal distribution and selected the best fit based on the lowest error.**

Comment 5: Line 140-142: Fitted size-distribution has been extrapolated on both tails of distribution. What is the observed range of the distribution? What is the extrapolation range? Have authors compared the extrapolated values with any observations? Further, 21-samples (3 minute per scan, line 118) running average is about 1-hour running average which can smoothen data significantly when observation is limited by 6 hours. Can you discuss in details?

Response: The observed range of the size distribution was 15.7 nm to 746.5 nm. We extrapolated up to 4 µm. We added text to the manuscript to clarify this and added example fits to the supplemental information. We also added clarification on how this approach is different from typical smog chamber wall-loss experiments (see response to reviewer comment 8, below).

As for comparing against smog chamber wall-loss methods, there the whole experiment time is typically used for a single time-invariant fit. Thus, our 21 samples (1-hour) running average is a higher resolution and required for our analysis.

This portion of Section 3 now reads:

Second, we fitted these observed rates to theoretical rates calculated from Particula (Particula et al., 2025), a python-based aerosol microphysics package. **The first step was to generate a new time series at a higher size resolution (log-spaced 250 bins), starting at 20 nm and extrapolating the 746 nm SMPS upper limit to 4 µm. The size-dependent particle rate was then computed as the linear slope of a 21-point moving window (10 before and 10 after). The time window (60 min) was chosen through iteration, as shorter than 20 min had too much noise to have self-consistent results and longer than 90 min had increasing fit residuals. Resulting in a smoothed time evolution, which was shown to be effective in coagulation analysis in Mahfouz and Donahue (2020a). Our moving window approach is different from smog chamber wall-loss experiments where the full 5 hours of the wall-loss experiment would be used to fit an apparent size-dependent, time-invariant wall-loss correction (Wang et al., 2018).**

Added Supplemental Information:

2.3 Example Distribution fits.

Examples of smoke, sucrose, and NaCl experiments of a distribution fit at the 2 hour experiment mark, accompanied by the Pearson R-squared fit for the experimental time used in the analysis.

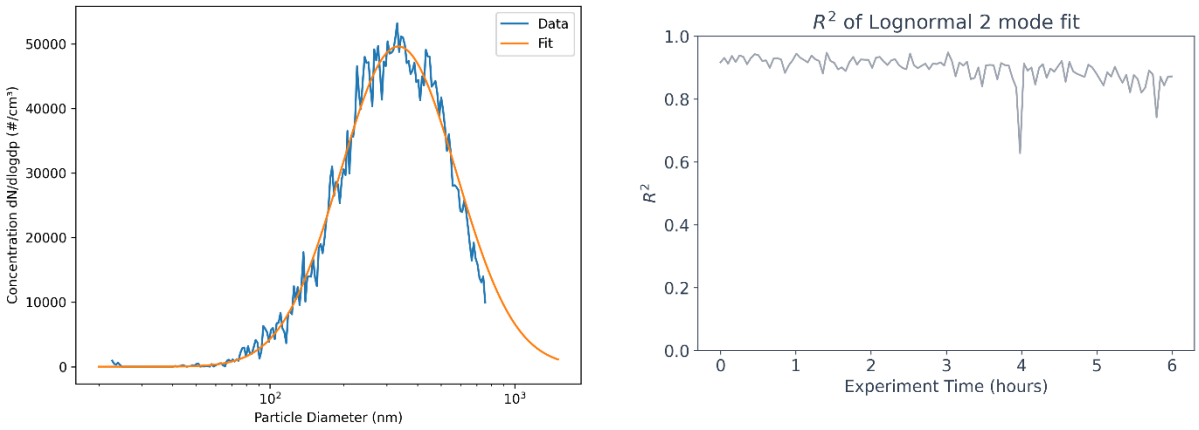

Figure S5: NaCl experiment. Left: fitted and measured size distribution. Right: Pearson R-squared of fit.

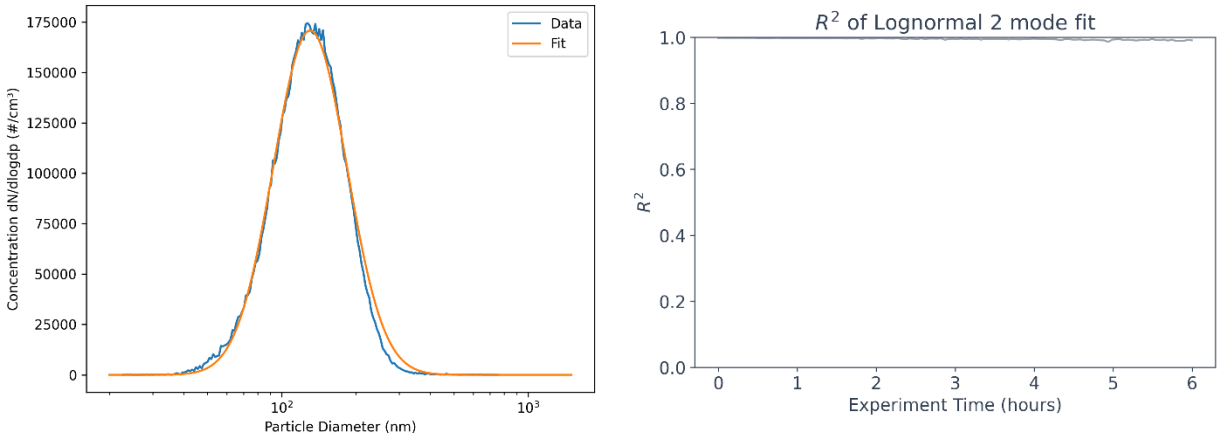

Figure S6: Smoke experiment. Left: fitted and measured size distribution. Right: Pearson R-squared of fit. Note the R-squared line is very close to 1 for most of this experiment.

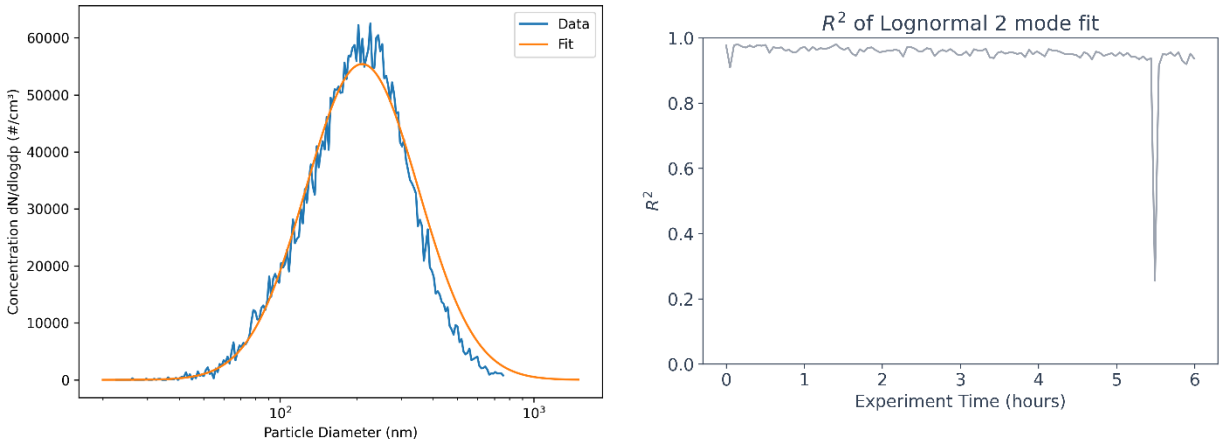

Figure S7: Sucrose experiment. Left: fitted and measured size distribution. Right: Pearson R-squared of fit.

Comment 6: In Fig. 4(a), there is significant drop in wall-eddy diffusivity between 4 and 5 hours for soot particles, before it increases again. Can authors explain the reason?

Response: We do not have a specific explanation for that change in the smoke experiments. There is a similar change in the NaCl experiments, dropping at 2.9 to 3.7 hr then higher at 3.7 to 4.6 hr.

Comment 7: Coagulation and wall-loss factor can be very different for cloud-chambers, because of wet walls and supersaturated conditions. What is the insights from current results that can be helpful for moist cloud-chamber?

Response: Our dry-wall experiments establish the usage of a physics-based size-dependent wall-loss coefficient and show that coagulation corrections depend on concentration (see response above). These experiments and error analysis let us target concentration ranges for just wall-loss vs. coagulation corrections, in the future. These target ranges are important when assessing additional processes introduced by humidity and supersaturation (e.g., enhanced deposition to wet surfaces or condensational growth). Using the same analysis framework on humid runs, any increase in the loss rate or redistribution of sizes can be quantified as a deviation from this dry baseline, directly isolating moisture-specific impacts.

Comment 8: There is a large literature on aerosol chambers, including wall-loss models and coagulation. This should be reviewed and the originality of this chamber should be discussed.

Response: We have updated the manuscript to include more details on previous chamber work including published reviews. We added context on the wall-loss correction compared to other methods used in smog chamber experiments.

Updated text on previous chambers:

Aerosol chambers are used to understand the chemical and microphysical transformation in controlled conditions (Becker, 2006; Doussin et al., 2023). Many were built for gas-phase and secondary organic aerosol experiments and feature large volumes with Teflon walls to reduce wall-losses (Hynes et al., 2005; Shao et al., 2022b). Others are optimized for specific aerosol processes, like bioaerosols (Massabo, 2018).

Cloud chambers are a class of chambers for investigating cloud microphysical mechanisms under well-controlled conditions (Chang et al., 2016; Khlystou et al., 1996; Niedermeier et al., 2020; Shao et al., 2022). Existing cloud chambers are their own institutional facility in the case of CLOUD at CERN (The Cloud Collaboration, 2001), AIDA Chamber EUROCHAMP (Wagner et al., 2006), and PI-chamber at MTU (Chang et al., 2016). **These types of facilities are critical for advancing science but are often oversubscribed and require significant support to operate.**

As outlined in many of the papers cited in the previous paragraph, all chambers however, come with artifacts—most notably, the loss of particles to chamber walls through gravity, diffusion, convection, and electrostatic forces (Corner and Pendlebury, 1951; Fotou and Pratsinis, 1993; Mahfouz and Donahue, 2020a; Wang et al., 2018).

Updated text on wall-loss:

Equation 2 shows the wall-loss rate (β) varies with particle size, derived from a rectangular-chamber formulation adapted from Crump and Seinfeld (1981) and Crump (1982). It incorporates both diffusion-driven transport and gravitational settling. In this formulation, L, W, and H denote the chamber's length, width, and height, respectively; k_e is the wall-eddy diffusivity (a free fit parameter); D is the particle diffusion coefficient; and v_p is the particle gravitational settling velocity. **This physics-based wall-loss coefficient is different from Wang et al. (2018) method of apparent size-dependent wall-loss fit. In the apparent size-dependent wall-loss fit the rate equation is a two-term first-order rate equation. In the apparent size-dependent wall-loss fit the rate equation is a two-term first-order rate equation, where there are no physical terms for the size of the chamber or particle settling velocity, in contrast to what we use in Equation 2. The apparent size-dependent wall-loss approach is common for smog chamber experiments (Doussin et al., 2023; Keywood et al., 2004; Loza et al., 2012; Nah et al., 2017; Ng et al., 2007) but would not work here since one of our goals is to specifically determine coagulation. In our case, we need a physics-based wall-loss rate equation to determine if there are any coagulation corrections that could be**

applied. If we had used the apparent size-dependent wall-loss fit, then there would be little to no residuals for a coagulation correction analysis.

Minor comments:

Comment 1: Line-183: Indicate the plot number in the supplement.

Response: We have made this update.

Comment 2: Line-201: Why does gravitational settling diminish over time as mixing subsides? Please include the reference here.

Response: During the revision we realized there was an error in the calculation. With the error fixed the gravitational settling no longer shows this trend. We have updated the text to reflect this correction: Over longer times (>1 hours), all three aerosol types converge toward similar wall-loss rates, in agreement with the literature indicating that chamber turbulence diminishes over time as mixing subsides.

Comment 3: Lines 91-93: Does dilution line affect the residence time in the chamber? How?

Response: No, it does not. Upon reflection we recognize that our discussion of the rate equation may have been confusing. In the experiments we push clean air into the chamber to get a sample out, we now call this the "chamber flow coefficient" (see below, which determines the residence time and is a dilution step of the aerosol inside the chamber). After the aerosol sample comes out there is a sample dilution step, so we have enough sample to be measured by all instruments and lowers the sample humidity when operating the chamber with humidity.

Updated text: The resulting size-dependent rate was subsequently used to fit the underlying aerosol processes in Equation 1 where $N(D_p)$ represents the number concentration of particles of diameter, D_p, K_{12} is the coagulation kernel, W_C^{-1} is the coagulation correction factor, N_1 and N_2 are the concentrations of particles in the bins for K_{12}, k_{flow} is the **chamber flow coefficient**, and β is the wall-loss rate.

The **chamber flow coefficient**, $k_{flow} = Q/V$, characterizes how the clean air flow rate (Q) is used to push sample flow out of the chamber volume (V).